Acta Pharmaceutica Sinica B 2026;16(8):5131−5147

Chinese Pharmaceutical Association
Institute of Materia Medica, Chinese Academy of Medical Sciences

Acta Pharmaceutica Sinica B

www.elsevier.com/locate/apsb
www.sciencedirect.com

ORIGINAL ARTICLE

CDK9 inhibition sensitizes intrinsically resistant *BRAF*^{V600E} mutant colorectal cancer to BRAF inhibitors

Ning Wei[a,b,c,*], Natalie Thielen[a,c,d], Mahshid Mohammadi[a,b,c], Muzaffer Ahmed Bhat[a,b,c], Terence Li[a,b,c], Yan Sun[d], Seiya Kitamura[a,d], Edward Chu[a,b,c,*], Chaoyuan Kuang[a,b,c,*]

[a]*Montefiore Einstein Comprehensive Cancer Center, Cancer Therapeutics Program, Albert Einstein College of Medicine, Bronx, NY 10461, USA*
[b]*Department of Oncology, Albert Einstein College of Medicine, Bronx, NY 10461, USA*
[c]*Department of Molecular Pharmacology, Albert Einstein College of Medicine, Bronx, NY 10461, USA*
[d]*Department of Biochemistry, Albert Einstein College of Medicine, Bronx, NY 10461, USA*

Received 9 September 2025; received in revised form 25 January 2026; accepted 27 January 2026

KEY WORDS

CDK9;
BRAF;
Drug resistance;
Drug combination;
Colorectal cancer

Abstract Recently, the BRAF inhibitor (Encorafenib) in combination with Cetuximab and mFOLFOX6 has been approved for the treatment of metastatic CRC (mCRC) patients with *BRAF*^{V600E} mutation in the first line. However, intrinsic resistance to BRAFi still limits its therapeutic efficacy, and the clinical response is only ∼5%. One potential strategy to improve mCRC therapy is to combine agents that target key cellular signaling pathways, which may yield synergistic antitumor efficacy and overcome drug resistance. Herein, CDK9 inhibitors (CDK9i) were identified as candidate synergistic agents through kinase library-based high-throughput screening (HTS) and RNA sequencing. CDK9i synergistically sensitizes the therapeutic efficacy of BRAFi (as well as inhibitors of well-known downstream effector of BRAF, MEK and ERK) in multiple intrinsically resistant CRC models. Notably, CDK9i in combination with BRAFi also resulted in an enhanced therapeutic response in chemo-resistant CRC cells and PDOs. Taken together, CDK9 inhibition overcomes intrinsic resistance to BRAFi monotherapy, and targeting CDK9-mediated transcriptional elongation appears to be a promising and tolerable sensitization strategy for BRAFi-based treatment in mCRC, even in chemo-resistant mCRC.

*Corresponding authors.
E-mail addresses: ning.wei@einsteinmed.edu (Ning Wei), chaoyuan.kuang@einsteinmed.edu (Chaoyuan Kuang), edward.chu@einsteinmed.edu (Edward Chu).

Peer review under the responsibility of Chinese Pharmaceutical Association and Institute of Materia Medica, Chinese Academy of Medical Sciences.

https://doi.org/10.1016/j.apsb.2026.05.008

1. Introduction

Colorectal cancer (CRC) remains the second-leading cause of cancer-related death in the world[1]. In the United States, it is estimated that 154,270 new cases and 52,900 deaths occurred in 2025[2]. Approximately 10% of CRC patients carry a *BRAF* mutation and this type of CRC is more aggressive and has poorer prognosis than other types[3]. Of note, *BRAF* mutation leads to a lack of benefit from standard chemotherapy[4,5]. The V600E mutation accounts for 95% of all *BRAF* mutations in CRC and is associated with female sex, right-side primary tumor, mucinous tumors, and increased metastasis[6-8]. Molecularly, *BRAF* ^{V600E} mutation causes activation of BRAF signaling cascade through BRAF monomer and in a RAS-independent manner[9]. Activation of its downstream effectors, including MEK and ERK is particularly strong[10]. Uncontrolled upregulation of downstream signaling forms a high activating capacity of the MAPK pathway, further increasing transcription of oncogenes and promoting tumor cellular differentiation, proliferation, survival, and resistance to apoptosis[11].

Currently, Encorafenib, Vemurafenib and Dabrafenib are the FDA-approved BRAFi for metastatic melanomas[12]; expectations were high when BRAFi monotherapy was investigated in *BRAF* ^{V600E} mutant mCRC. Unfortunately, there was a lack of benefit and poor response to BRAFi alone in patients with *BRAF* ^{V600E} CRC[13]. Molecularly, the activation of *p*-EGFR is responsible for resistance to BRAFi monotherapy in mCRC[14]. This led to the investigation and approval of the combination of Encorafenib (BRAFi) and Cetuximab (EGFRi) for chemotherapy resistant *BRAF* ^{V600E} mutant mCRC[15]. While the triplet combination of Encorafenib, Cetuximab, and Binimetinib (MEKi) showed a similar OS and PFS as the Encorafenib and Cetuximab doublet, the triplet led to slightly higher rates of adverse events, leading to approval of the doublet[16,17]. Most recently, the FDA approved BRAFi (Encorafenib) in combination with Cetuximab and mFOLFOX6 (Fluorouracil, Leucovorin, and Oxaliplatin) for the treatment of patients with newly diagnosed *BRAF* ^{V600E} mCRC[18,19]. However, a proportion of mCRC patients remain intrinsically resistant to BRAFi, and some patients who initially respond will subsequently acquire resistance to BRAFi during the treatment. In the BREAKWATER study, nearly 50% of patients progressed on Encorafenib plus Cetuximab and chemotherapy within a year[20]. Due to intrinsic resistance to BRAFi, other *BRAF* inhibitors such as Dabrafenib in combination with Trametinib is not beneficial for refractory mCRC[21].

Due to the pervasiveness of drug resistance, it is urgent to discover novel agents for sensitizing BRAFi in mCRC. Therefore, we conducted a high-throughput screen of a kinase library to determine the best compounds to synergize with BRAFi. CDK9 was identified as a promising candidate target. CDK9, a global regulator of transcription, impacts multiple oncogenic transcriptional networks, and is a promising target in MYC-driven tumors, such as CRC[22]. Hsu's group[23] identified that co-inhibition of CDK2 and CDK9 can serve as a novel combinatorial therapy to the treatment of CRC. In ongoing work in our lab, we found that CDK9 inhibitors suppressed the transcription of several MAP kinase signaling molecules. Given the promising therapeutic effect of CDK9 inhibitors and mechanism of action, it is conceivable that CDK9i in combination with BRAFi may lead to synergistic antitumor activity against *BRAF* mutant mCRC. Therefore, the combinational effect of BRAFi (Encorafenib and Dabrafenib) and 3 clinically promising CDK9i (AZD4573, NVP2, BAY1251152) were investigated in *in vitro* and *in vivo* CRC models with pV600E mutation.

2. Materials and methods

2.1. Chemicals and reagents

BRAF inhibitors (Encorafenib and Dabrafenib), 3 well-characterized CDK9 inhibitors (AZD4573, NVP2, BAY-1251152), MEK inhibitors (Binimetinib, Trametinib), ERK inhibitors (ASN007, Ravoxertinib), and the kinase library (Supporting Information Table S1) were purchased from MedChemExpress LLC. CDK9 siRNA (h) (sc-29268) was purchased from Santa Cruz (Dallas, TX). All other chemicals were obtained from Sigma−Aldrich Chemical Co. (St. Louis, MO, USA).

2.2. Cell culture and cell lines

HCT116, RKO, LS513, SW1463, HT-29, Colo205, CCD-841 CoN cells were purchased from the American Type Culture Collection (ATCC, Manassas, VA, USA). HCT116 BRAF pV600E cells were obtained from GeneCopoeia, Inc., (Rockville, MD, USA). RKO-5FUR10 cells were gifted from Drs. Schmitz and Liu from UPMC Hillman Cancer Center[24]. All cells were maintained in RPMI-1640 (ATCC, Manassas, VA) with 10% (*v*/*v*) fetal bovine serum (FBS) (Gemini Bio-Products; Sacramento, CA, USA) at 37 °C in a humidified incubator with 5% CO_2. Cell lines were authenticated by human STR profiling performed by the Genomics Core at the Albert Einstein College of Medicine. Cells were monitored every 2 months for the mycoplasma with Myco-Sniff-Valid (MP Biomedicals, MP093050301; Lot ID: U1124283604).

2.3. High-throughput screening (HTS)

RKO cells were seeded into black CELLSTAR® uCLEAR® 384-well plates (Greiner, Monroe, NC, USA) at a density of 1000 cells/well. The kinase inhibitors were re-suspended as 20 μmol/L stock solutions, and 0.1 μL was dispensed into the 384-well plates using a BRAVO liquid handler (Agilent, Santa Clara, CA, USA) in a randomized plate layout to control for plate effects. All kinase inhibitors were tested at 50 nmol/L with and without Encorafenib (300 nmol/L). After 72 h, 20 μL of CellTiter-Glo reagent (Promega #G9241) was added to each well. The 384-well plate was placed in BioTek Cytation 5 (Agilent, Santa Clara, CA, USA), followed by gentle mixing for 2 min, and luminescence was measured using relative luminescence units (RLUs).

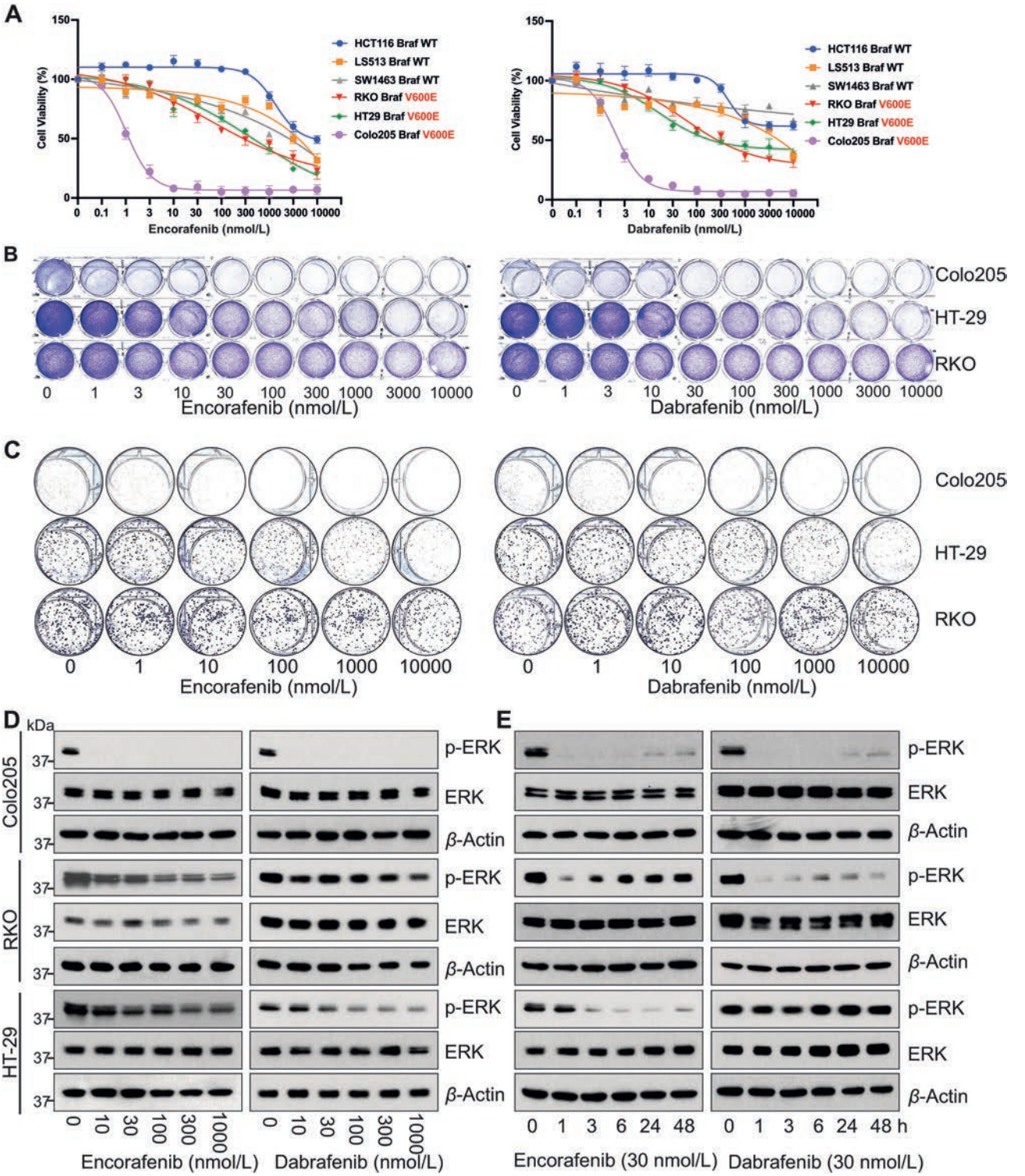

Figure 1 RKO and HT-29 cells exhibit intrinsic resistance to BRAFi monotherapy. (A) The effect of BRAFi (Encorafenib and Dabrafenib) on the growth of colon cancer cells, including Colo205, RKO, HT29 with $BRAF^{V600E}$ mutation, and HCT116, SW1463, LS513 with wild-type *BRAF*. The CRC cells were treated with BRAFi for 72 h, and the cell viability was determined by MTS assay. (B) The efficacy of BRAFi in suppressing the growth of $BRAF^{V600E}$ mutant CRC cells. Colo205, RKO, and HT-29 cells were seeded into 12 well plates and then exposed to BRAFi for 48 h. The living cells were stained by crystal violet. (C) The cytotoxic effect of BRAFi on clonogenic growth. 400 cells/well were seeded into the 6-well plates and then treated with BRAFi for 24 h. Fresh medium was exchanged every 3−4 days, and after 10−14 days the clones were stained by crystal violet. (D, E) the therapeutic efficacy of BRAFi on blocking p-ERK signal. Colo205, RKO, and HT-29 cells were treated with BRAFi alone with various dosing and timing, the p-ERK, ERK, and β-actin were determined by immunoblot analysis. A representative image from 3 to 5 independent experiments is shown.

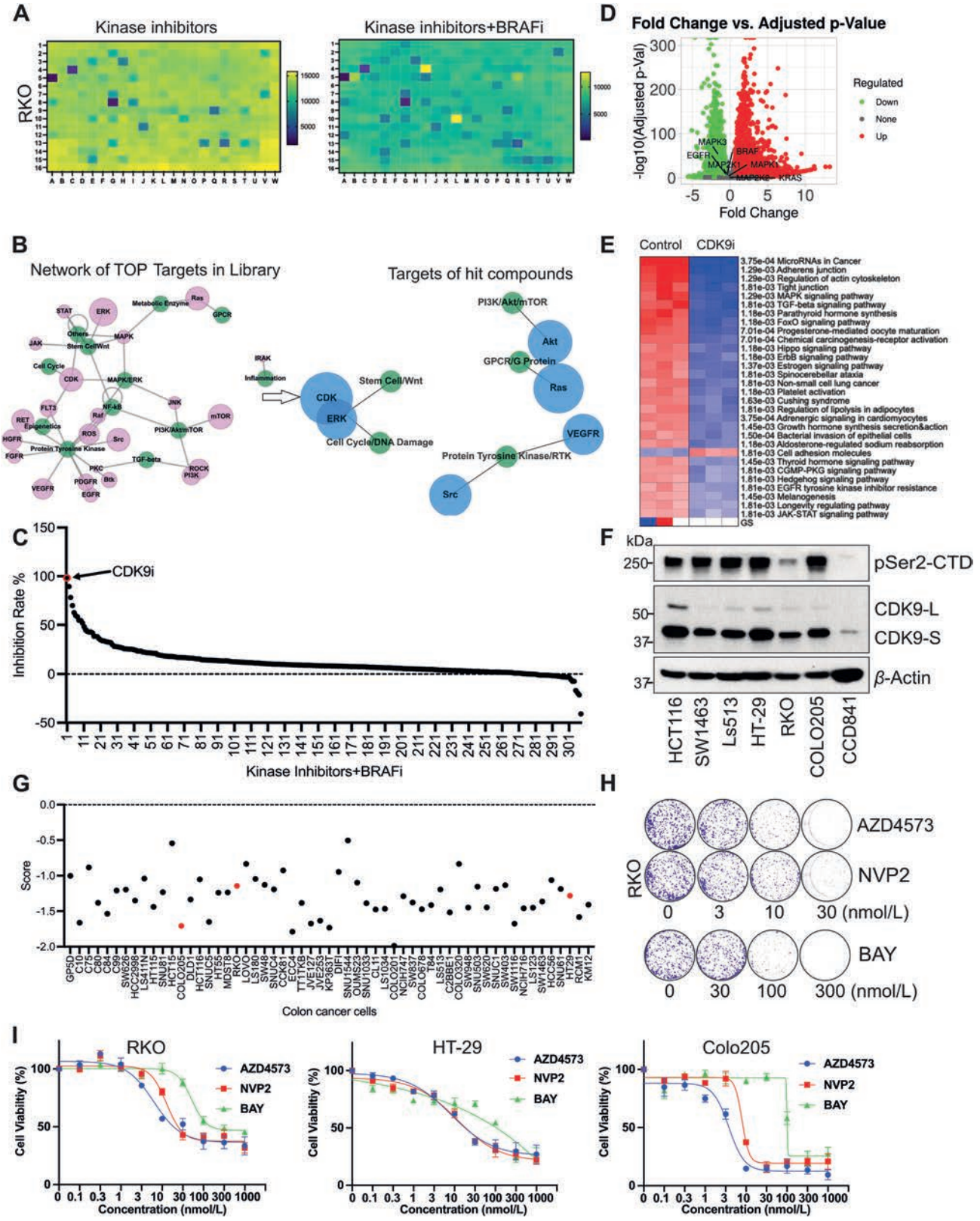

Figure 2 CDK9 was discovered as a candidate target by using high-throughput screening. (A) Kinase library screening was performed by HTS. (B) Network Cluster graph of the kinase library compared to the top hit compounds. Cluster nodes size based mean inhibition percentage in library screen. Each pathway (green) and target (pink) ($k = 0.7$) compared to the top hit targets (blue) ($k = 0.5$). (C) CDK9 inhibitor is the most potent candidate agent for enhancing the efficacy of BRAFi. (D, E) RNA-seq data showed that CDK9i suppresses the MAPK pathway, including *BRAF*, *MAPK3*, *MAP2K1*, *MAPK1*, *KRAS* and *EGFR*. RKO cells were treated with NVP2 (30 nmol/L) for 24 h, and RNA-seq was performed. (F) The protein expression level of CDK9 and phosphorylation (ser2) of RNA polymerase II in human CRC cell lines (HCT116, RKO, HT-29,

2.4. Cell growth assay

Cell viability was determined by the MTS assay (Promega #G5430). The CRC cells were plated in 96-well plates. On the following day, cells were treated with various concentrations of BRAFi (Enco or Dabr) for 72 h. The IC_{50} value of each compound was calculated by GraphPad Prism 9.0 software. According to the IC_{50} of a single drug, cells were treated with CDK9i in combination with BRAFi, MEKi and ERKi for 72 h, CalcuSyn software (version 2.0, Biosoft, Cambridge, UK) was used to calculate the combination index (CI).

Crystal violet staining assay: human CRC cells were seeded into a 12-well plate at a density of 1.25×10^5 and then treated with BRAFi and/or CDK9i for 48 h, the living cells were stained with crystal violet. Clonogenic assay: human CRC cells were seeded in 6-well plates at a density of 400 cells/well. On the following day, cells were treated with various concentrations of BRAFi for 24 h, the growth medium was replaced every 3−4 days. After 10−14 days, clones were fixed with crystal violet for 30 min, washed, and air-dried before counting clones >50 cells.

2.5. Apoptosis assay

As previously described[25], RKO cells were treated with Encorafenib/Dabrafenib (300 nmol/L) and/or NVP2 (30 nmol/L) for 24 h. The apoptotic cells were determined by FITC Annexin V Apoptosis Detection Kit (BD Biosciences; San Jose, CA, USA), and analyzed on the Flow Cytometer (Cytek Aurora analytical flow cytometer) at Flow Cytometry Core Facility of the Albert Einstein College of Medicine.

2.6. Immunoblot analysis

Immunoblot analysis was performed as previously described[26]. The detailed information of primary antibodies was listed in Supporting Information Table S2. Signal intensities were quantified by using Image J software. Relative protein expression was normalized by β-actin or GAPDH expression.

2.7. Human colorectal cancer organoid culture

Human colon cancer organoid (*BRAF* ^{V600E}: #CK9677-ID-624824-186-R; #CK7719-ID-282377-053-R; #CK8485-ID-857933-349-R; #CK8911-ID-616215-338-R) was obtained from NCI, and another CRC organoid (#CRC-22-007, *BRAF* WT; #CRC-22-008, *BRAF* WT) was generated in our lab (Einstein IRB# 2021-13730). The detailed information for CRC organoid culture is listed in Supporting Information Table S3 and the Supporting Information (methods).

2.8. Cell Titer-Glo 3D cell viability assay

According to our previous protocol[26], the viability of the PDOs were determined by CellTiter-Glo® 3D Reagent (Promega G9683). Luminescence was detected by the FLUOstar Omega microplate reader (BMG Labtech).

2.9. RNA sequencing

RKO cells were treated with CDK9i (NVP2 30 nmol/L), and the total RNA was extracted using the Direct-zol RNA MiniPrep Kit (Zymo Research, Cat #R2071). RNA concentration and purity were evaluated using a NanoDrop 2000 (ThermoFisher). RNA sequencing was performed by Novogene (Sacramento, CA, USA) for analysis.

2.10. Reverse-phase protein array (RPPA)

As previously described[25], RKO cells were treated with NVP2 (30 nmol/L) and/or Encorafenib (300 nmol/L) for 24 h, the cells were harvested, and protein lysates were prepared. RPPA was performed by the Functional Proteomics RPPA Core Facility at the MD Anderson Cancer Center (Houston, TX, USA) for analysis.

2.11. RKO xenograft mice model

Animal experiments were approved by the Institutional Animal Care and Use Committee at the Albert Einstein College of Medicine (protocol #00001618, approved on 1/5/2023). RKO cells (5×10^6) were counted using trypan blue for viability, prepared as single cell suspension in 0.2 mL of PBS, and implanted subcutaneously on the flank of athymic nude female mice (6−8 weeks). Once tumor volume reached ∼100 mm^3, mice were randomized to 4 groups (5 mice/group): (1) Control (10% DMSO + 90% (20% SBE-β-CD in Saline)); (2) Encorafenib (10 mg/kg); (3) NVP2 (8 mg/kg); (4) Combination group. Tumor volume was calculated according to Eq. (1):

$$\text{Tumor volume} = (L \times W \times W)/2 \quad (1)$$

where L and W represent the length and width of the mice tumor. Tumor volume and body weight were measured 3 times/week. Animals were sacrificed on Day 20, 2 h after the last drug treatment. Tumors were snap-frozen in liquid nitrogen and stored at −80 °C. IHC staining for TUNEL, Ki-67 and p-ERK were performed in Albert Einstein Histology and Comparative Pathology core, and the Ki-67 positive percentage was calculated by image J.

2.12. Patient-derived xenograft

PDX tissue (#MA1119-ID-624824-186-R, *BRAF* ^{V600E}; #CM0050-ID-234829-215-T, *BRAF* WT) was obtained from the NCI Patient-Derived Models Repository (PDMR). According to NCI protocol, the tumor tissues were implanted into NOD-SCID mice (6−8 weeks). Using passage 3, the PDX tumor tissues were harvested and expanded. When the tumor size reached 200−300 mm^3, the mice were divided into 4 groups, including (1) Control group; (2) NVP2 (8 mg/kg); (3) Encorafenib (10 mg/kg);

Colo205, LS513, LS174T and CCD841 cells) were determined by immunoblot analysis. (G) The perturbation effect of CDK9 inhibition on the proliferation of human CRC cells. (H) The effect of CDK9i on clonogenic growth. 400 cells/well were seeded into the 6-well plate, and then treated with CDK9i (AZD4573, NVP2 and BAY) for 24 h. After 10−14 days, clones (>50 cells) were fixed, stained by crystal violet, and manually counted. A representative of 3−5 experiments is shown. (I) Effect CDK9i on the growth of CRC cells. RKO, HT-29 and Colo205 cells were treated with CDK9i for 72 h, cell viability was determined by MTS assay, and the IC_{50} was calculated by GraphPad Prism 9.0 software. Values represent the mean ± SD from 3 to 5 independent experiments.

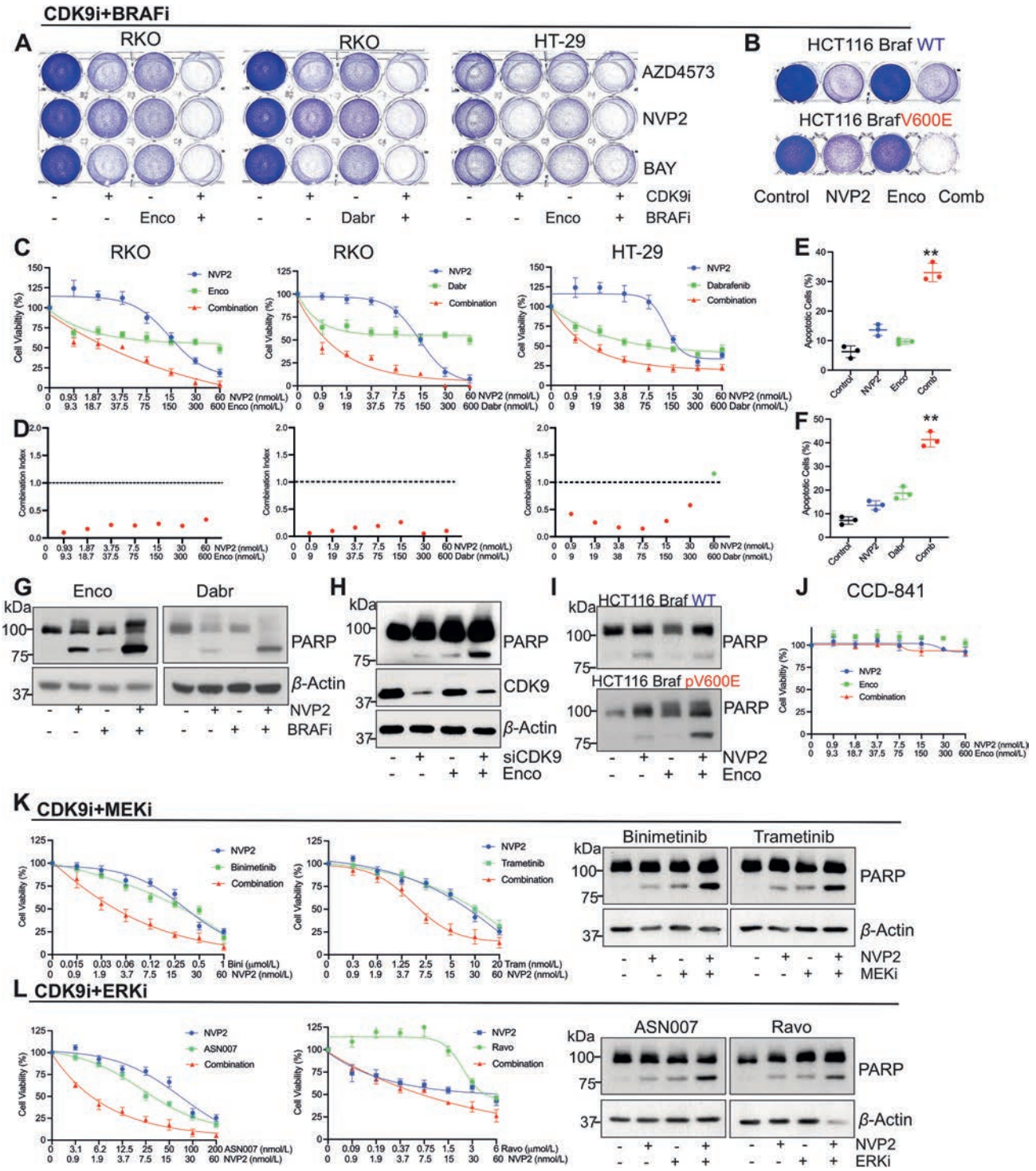

Figure 3 The synergistic effect of CDK9i in combination with BRAFi, MEKi and ERKi in intrinsically resistant CRC cells. (A) The synergistic effect of CDK9i and BRAFi on the proliferation of *BRAF*^{V600E} mutant human CRC cells. RKO and HT-29 cells were treated with CDK9 inhibitors (AZD4573, 10 nmol/L; NVP2, 30 nmol/L; BAY, 100 nmol/L) and/or BRAFi (Encorafenib; Dabrafenib, 300 nmol/L) for 48 h, then the living cells were stained by crystal violet. A representative of 3−5 experiments is shown. (B) Knock-in of *BRAF*^{V600E} restores the synergistic effect of CDK9i and BRAFi on the growth of HCT116 cells. HCT116 cells with *BRAF*^{V600E} mutation and parental cells were seeded in 12-well plate and treated with CDK9i and/or BRAFi for 48 h, and the living cells were stained by crystal violet, with a representative of 3−5 experiments shown. (C) The synergistic effect of CDK9i and BRAFi on the growth of *BRAF*^{V600E} mutant human CRC cells. RKO or HT-29 cells were seeded in 96-well plates and then treated with different concentrations of CDK9i (NVP2, AZD4573, BAY) and/or BRAFi for 72 h. Cell growth was determined by the MTS assay. (D) Data from 3 to 5 independent experiments were used to calculate the Combination Index (CI) according to the Chou-Talalay method. (E, F) CDK9i enhances the efficacy of BRAFi on inducing apoptosis. RKO cells were exposed to CDK9i and/or BRAFi for 24 h, the apoptotic cells were measured by flow cytometry. (G) RKO cells were treated with CDK9i and/or BRAFi for 24 h, the cleaved PARP were

(4) NVP2+Encorafenib. Tumor volumes and body weight were monitored 3 times/week. Mice bearing #MA1119 tumor of the control group were sacrificed on Day 13, and other mice were sacrificed on Day 20, 2 h after the last drug treatment. Tumors were snap-frozen in liquid nitrogen and stored at −80 °C. IHC staining for TUNEL, Ki-67 and p-S6 were performed in Albert Einstein Histology and Comparative Pathology core. Tumor tissues were used for immunoblot analysis. Mice bearing *BRAF* WT (CM0050) tumors were treated with NVP2 and/or Encorafenib for 30 days. The tumor size and body weights were monitored every other day.

2.13. Statistical analysis

All experimental data are presented as mean ± standard deviation (SD). Statistical analysis was performed using SPSS software (Version 16.0). The Student's *t*-test (two-tailed) was used for two group comparisons. One-way ANOVA with Tukey's HSD *post hoc* test was used for comparisons between groups of more than two unpaired values. $P < 0.05$ was considered statistically significant.

3. Results

3.1. RKO and HT-29 cells exhibit intrinsic resistance to BRAFi monotherapy

To compare the sensitivity and selectivity of BRAFi against human CRC cells, 3 CRC cells with *BRAF* ^{V600E} (Colo205, RKO, HT-29 cells) and 3 CRC cells with wild-type *BRAF* (LS513, HCT116 and SW1463 cells) were used to determine the cytotoxicity of Encorafenib and Dabrafenib. As shown in Fig. 1A and Supporting Information Table S4, Colo205 cells exhibit more sensitive to BRAFi than RKO and HT-29 cells. The IC_{50} of BRAFi alone in Colo205 cells is approximately 1 nmol/L; while the IC_{50} of BRAFi in RKO and HT-29 cells is 300−400-fold higher than that in Colo205 cells (RKO = 309.8 ± 12.4 nmol/L; HT-29 = 398.1 ± 9.8 nmol/L); this result suggests that RKO and HT-29 cells harbor intrinsic resistance to BRAFi. Meanwhile, the IC_{50} value of *BRAF* wild-type CRC cells is over 10,000 nmol/L, showing that the BRAFi were selective against *BRAF* ^{V600E} mutant CRC cells. We further confirmed the sensitivity of BRAFi in Colo205, RKO, and HT-29 cells by using crystal violet assay. As shown in Fig. 1B, 1−3 nmol/L of BRAFi significantly suppressed the growth of Colo205 cells. Of note, 10,000 nmol/L of BRAFi could not fully suppress the growth of RKO and HT-29 cells. In addition to the MTS and crystal violet assay, colony formation assay was performed to validate the sensitivity of BRAFi in these CRC cells. As seen in Fig. 1C, Colo205 clone formation was significantly reduced as compared to RKO and HT-29 cells, which is consistent with their relative IC_{50} and cell survival result. Given that p-ERK is the key downstream effector of BRAFi, the ability of BRAFi to inhibit p-ERK in CRC cells can be related to their sensitivity. Consistently, BRAFi alone potently and continuously suppressed the activation of ERK in Colo205 cells. 10 nmol/L of BRAFi almost completely blocked the p-ERK signal (Fig. 1D and E). In contrast, ∼50% of p-ERK was suppressed by 1000 nmol/L of BRAFi in RKO and HT-29 cells. Meanwhile, the feedback activation of ERK was observed in RKO cells after 6 h of exposure to BRAFi. Thus, BRAFi alone could not effectively or durably turn off p-ERK in RKO and HT-29 cells. Restoration of p-ERK signal during long-term BRAFi exposure could be responsible for the intrinsic resistance against BRAFi.

3.2. CDK9 was discovered as a candidate target by using high-throughput screening

The rational combination strategy is a promising approach to improve the efficacy of BRAFi and overcome drug resistance. Thus, high-throughput screening (HTS) of the kinase inhibitor library was used for the discovery of candidate agents overcoming BRAFi intrinsic resistance. In total, over 300 kinase inhibitors alone or in combination with BRAFi (Encorafenib) were screened (Fig. 2A). In addition to the expected finding of EGFRi, FGFR2i, and ERKi, CDK9i exhibited the strongest synergistic effect in combination with BRAFi (Fig. 2B). The inhibitory rate of this combination on cell growth reached ∼98% (Fig. 2C). CDK9 is a global regulator of transcriptional elongation and a key node in multiple oncogenic transcriptional networks, making it a promising target in a variety of transcriptionally addicted cancers, especially in MYC-driven tumors such as CRC. CDK9, a Ser/Thr kinase, belongs to the family member of CDKs (Supporting Information Fig. S1). RNA sequencing data suggests that CDK9i suppressed the MAPK pathway ($P = 0.00129$), including *BRAF*, *MAPK3*, *MAP2K1*, *MAPK1*, *KRAS* and *EGFR* (Fig. 2D and E). In human CRC cells, the mRNA level of CDK9 is widely expressed (Supporting Information Fig. S2). The protein expression level of CDK9 and phosphorylation (ser2) of RNA polymerase II in CRC cells is much higher than that in normal human colon epithelial cells (Fig. 2F). Moreover, the perturbation effect of CDK9 leads to suppression of CRC cell growth (the score<−1; Fig. 2G). Notably, 3 well-characterized CDK9i significantly reduced the clone number of RKO cells (Fig. 2H). In addition to colony formation suppression, the MTS cell growth assay showed that the CDK9i had potent cytotoxicity at low nmol/L level (AZD [∼10 nmol/L]>NVP2 [∼30 nmol/L]> BAY [∼100 nmol/L], in Fig. 2I). Overall, CDK9i appear to be promising therapies for *BRAF* ^{V600E} mutant CRC.

3.3. The synergistic effect of CDK9i and BRAFi in intrinsic resistance CRC cells

Our kinase inhibitor HTS and RNA-seq data suggested that CDK9i could sensitize intrinsically BRAFi-resistant CRC cells. To test the potential synergy between CDK9i and BRAFi, RKO or HT-29 cells were incubated with CDK9i and/or BRAFi for 48 h, and the living cells were stained by crystal violet. As shown in Fig. 3A. CDK9i in combination with BRAFi led to a stronger

determined by immunoblot analysis. (H) CDK9 knockdown enhance the effect of BRAFi on inducing cleaved PARP. (I) *BRAF*^{V600E} knock-in restore the synergistic effect of CDK9i and BRAFi on inducing programmed cell death. (J) Non-cytotoxic effect of CDK9i and/or BRAFi on the growth of normal human colon epithelial cells. (K, L) CDK9i enhanced the efficacy of MEKi and ERKi. RKO cells were treated with CDK9i and/or MEKi (Binimetinib or Trametinib)/ERKi (ASN007 or Ravo) for 72 h, the cell growth was determined by MTS assay. The cells were treated with CDK9i and/or MEKi/ERKi for 24 h, then cleaved PARP and β-actin were determined by immunoblot analysis. Values in the graph represent the mean ± SD from 3 to 5 independent experiments. $^{**}P < 0.01$, *vs.* control.

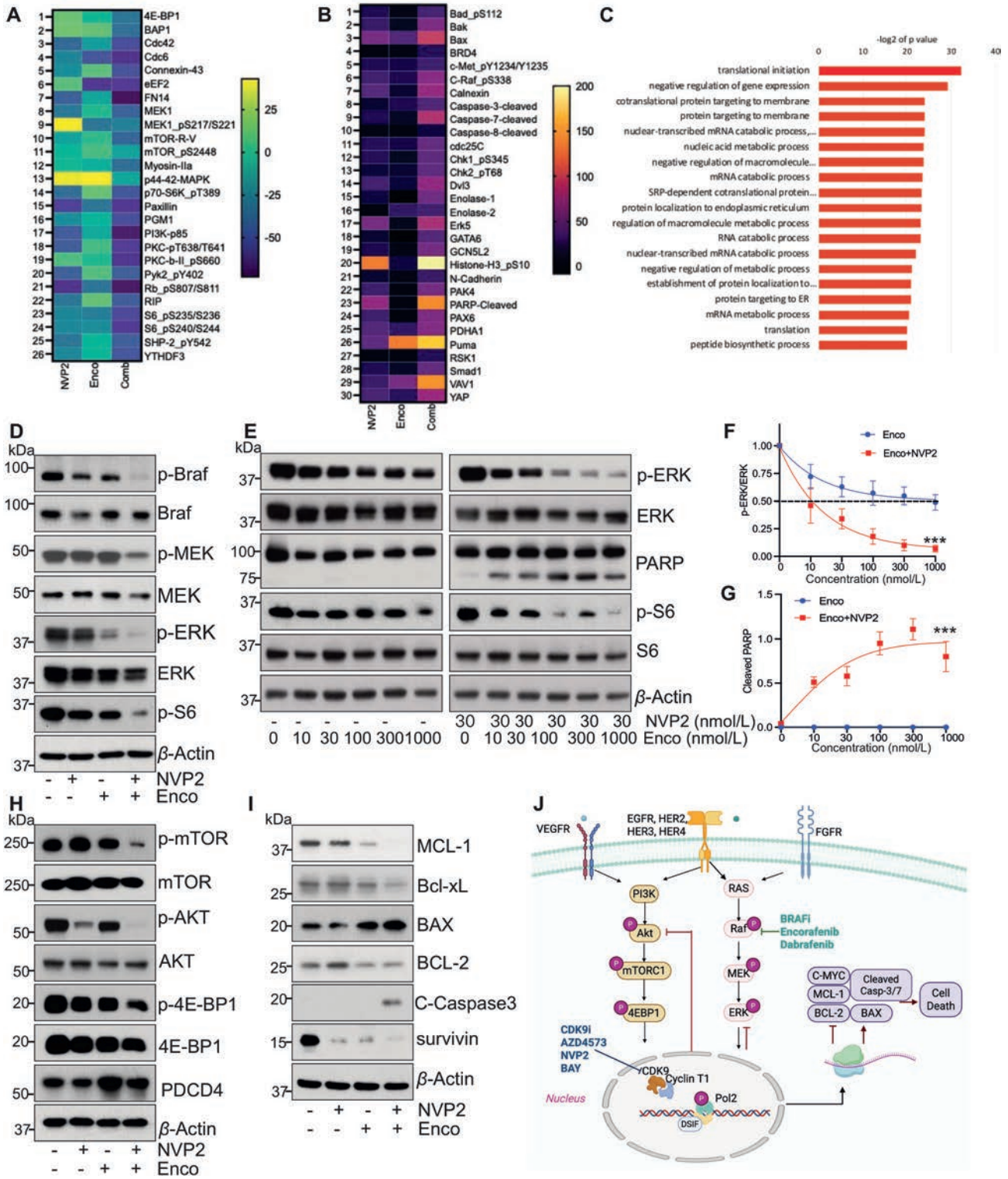

Figure 4 CDK9i synergistically blocked multiple cancer signaling pathways and enhanced the therapeutic response of BRAFi. (A) The down-regulated target proteins in the cancer signaling network after treatment with CDK9i and BRAFi. RKO cells were treated with NVP2 (30 nmol/L) and/or Encorafenib (300 nmol/L) for 24 h, then cell lysis was performed for RPPA analysis. (B) The up-regulated target proteins in cancer signaling network after exposure to CDK9i in combination with BRAFi. (C) The effect of this combination on the alteration biological processes in human cancer. (D) The synergistic effect of CDK9i and BRAFi on inhibition of BRAF/MEK/ERK/S6 pathway. (E−G) CDK9i enhances the efficacy of BRAFi on blocking p-ERK/p-S6 and inducing cleaved PARP. (H) The synergistic effect of CDK9i and BRAFi on suppression of AKT/mTOR/4 EB-P1 pathway. (I) CDK9i enhances the effect of BRAFi on mitochondria-mediated cellular apoptosis in intrinsic resistance CRC cells. (J) Signaling pathways altered by the combination of CDK9i and BRAFi (Created in BioRender. Wei, N (2026) https://BioRender.com/m2l5b57).

cytotoxic effect than single agent alone. This suggests that there is a potent synergistic effect of CDK9i and BRAFi. To confirm that the synergy of this combination is associated with BRAF mutant status, the parental HCT116 BRAF WT cells were genetically edited by using CRISPR-Cas9 to knock-in mutant *BRAF* ^{V600E} (Supporting Information Fig. S3). The synergistic effect of this combination was only observed in HCT116 BRAF ^{V600E} cells, but not in the parental cells (Fig. 3B). In addition to the cell survival assay, the synergistic effect of CDK9i and BRAFi on the growth of RKO or HT-29 cells was determined by MTS assay and the combination index (CI) was calculated by Chou-Talalay method. As seen in Fig. 3C and D, Supporting Information Figs. S4−S6, CDK9i (AZD4573, NVP2 and BAY) significantly sensitized the efficacy of BRAFi (Encorafenib and Dabrafenib), and had a strong synergy CI value (<0.5)[27]. To further quantify the cytotoxic effect of this combination, induction of early and late apoptotic cells by treatment of CDK9i (NVP2) and BRAFi (Encorafenib and Dabrafenib) was determined by flow cytometry. CDK9i markedly enhanced the efficacy of BRAFi on inducing apoptotic cells (Fig. 3E and F, Supporting Information Fig. S7). Cleaved PARP is an early marker of cells undergoing apoptosis. Consistently, the co-treatment of CDK9i and BRAFi yields a greater effect on the elevation of cleaved PARP in both RKO and HT-29 cells (Fig. 3G and Supporting Information Fig. S8). To genetically validate CDK9 inhibition as a sensitizer to BRAFi, the knock-down of CDK9 using siRNA significantly enhances the effect of BRAFi on the induction of cleaved PARP (Fig. 3H). Conversely, we also compared the effect of CDK9i plus BRAFi on inducing apoptosis in *BRAF* ^{V600E} HCT116 cells *versus* HCT116 BRAF WT parental cells. Consistent with our cell survival assay, the synergetic increase of cleaved PARP was only shown in the *BRAF* mutant HCT116 cells and not in the *BRAF* WT cells (Fig. 3I). Given the enhanced cytotoxic effect of this combination in CRC cells, the toxic effect of CDK9i and/or BRAFi on the growth of normal human colon epithelial cells was investigated. As seen in Fig. 3J, after 7 days of treatment, CDK9i and BRAFi alone or in combination did not affect the growth of the CCD-841 cells. MEK and ERK kinases are key downstream effectors of BRAF kinase, and it is possible that CDK9i could also enhance the efficacy of MEKi/ERKi. With this in mind, we investigated the combination of CDK9i with Binimetinib, Trametinib (MEKi); ASN007, or Ravo (ERKi) in *BRAF* pV600E RKO cells. As seen in Fig. 3K and L, CDK9i significantly enhanced the cytotoxic effect of MEKi and ERKi, and sensitized the ability of MEKi/ERKi on inducing cleaved PARP. Meanwhile, the BRAFi in combination with MEKi were used as a positive control, and a strong synergistic effect of this drug combination on the growth of RKO cells was shown (Supporting Information Fig. S9). These results suggest that CDK9i synergistically improved the therapeutic efficacy of BRAFi, MEKi and ERKi in CRC models.

3.4. CDK9i synergistically blocked multiple cancer signaling pathways and enhanced the therapeutic response to BRAFi

To clarify the synergistic mechanisms of CDK9i and BRAFi, approximately 500 cancer-related target proteins were screened by RPPA. As shown in Fig. 4A and B, 56 target proteins were significantly altered (cut-off value set at ∼30%), including 26 target proteins that were down-regulated and 30 target proteins that were up-regulated. These altered targets are involved in multiple cellular biological processes, such as translation initiation and negative regulation of gene expression (Fig. 4C). Moreover, CDK9i synergistically blocked multiple cancer survival signaling pathways and enhanced mitochondria-mediated apoptosis pathways. Of note, MEK/ERK/S6; PI3K/AKT/mTOR/4E-BP1; BCL2 family members and Caspase-3/7 were significantly suppressed by co-treatment. To validate the synergistic effect of this combination on RAF/MEK/ERK/S6 pathway, RKO cells were treated with CDK9i and BRAFi for 24 h, and the changes in target proteins were determined by immunoblot analysis. The activation of *BRAF*, MEK, ERK, and S6 were synergistically suppressed by this drug combination, validating our RPPA data (Fig. 4D). Furthermore, the CDK9i effectively enhances the ability of BRAFi to block p-ERK and induce cleaved PARP (Fig. 4E−G). In addition to BRAF/MEK/ERK/S6 pathway, PI3K/AKT/mTOR/4E-BP1 pathway was also synergistically suppressed, as shown through decreased p-AKT, p-mTOR and p-4E-BP1 (Fig. 4H). Finally, this drug combination resulted in a greater effect on inducing apoptosis, leading to reductions in the anti-apoptosis proteins MCL1, BCL-2, Bcl-xL and survivin, while the pro-apoptosis proteins BAX and active caspase3 were elevated (Fig. 4I and Supporting Information Fig. S10). Taken together, CDK9i significantly enhances the efficacy of BRAFi through inhibition of RAF/MEK/ERK/S6 and AKT/mTOR/4E-BP1 pathways in *BRAF* ^{V600E} mutant CRC (Fig. 4J).

3.5. CDK9i enhances the efficacy of BRAFi in CRC PDO with BRAF^{V600E} mutant, but not in BRAF WT PDO

To accelerate the translational investigation of the combination of CDK9i and BRAFi, and to validate the synergistic therapeutic efficacy in clinically relevant CRC models, CRC patient-derived organoids (PDOs) were treated with CDK9i and/or BRAFi, including 4 BRAF ^{V600E} mutant PDOs (CK9677; CK7719; CK8485; CK8911) and 3 wild-type *BRAF* (CRC-22-008; CRC-22-007; CK10278) PDOs. Using CK9677, a *BRAF* ^{V600E} mutant PDO, Ki-67 (cell proliferation marker), active caspase3 (apoptosis biomarker) and p-ERK (key downstream effector for BRAFi) were measured by IHC staining. As shown in Fig. 5A, the CDK9i in combination with BRAFi resulted in a decrease of Ki-67 and p-ERK positive staining, along with an increase of active caspase3 staining. The Ki-67 positive staining in drug combination was reduced to 15.5%, as compared to the control (50.8%). The p-ERK signal was markedly decreased (49.5% in control *vs.* 3.7% in combination). Moreover, the active caspase-3 positive stanning was synergistically induced by the NVP2 in combination with Encorafenib (NVP2 = 27.1% *vs.* Encorafenib = 10.2% *vs.* Combination = 55.7%). The size of PDOs in the combination group are smaller than CDK9i or BRAFi alone. To quantify the synergy between CDK9i and BRAFi, PDO viability was determined by CellTiter Glo 3D. CDK9i (NVP2) or BRAFi (Encorafenib) alone exerts a moderate cytotoxic effect on the growth of

The combination of CDK9i and BRAFi leads to synergistic inhibition of oncogenic signaling pathways, including BRAF/MEK/ERK/S6, AKT/mTOR/4E-BP1, and induction of mitochondria-mediated apoptosis. All protein expression levels of targets were determined by immunoblot analysis. A representative image from 3 to 5 independent experiments is shown. Values in the graph represent the mean ± SD from 3 to 5 independent experiments. ***$P < 0.001$ *vs.* control.

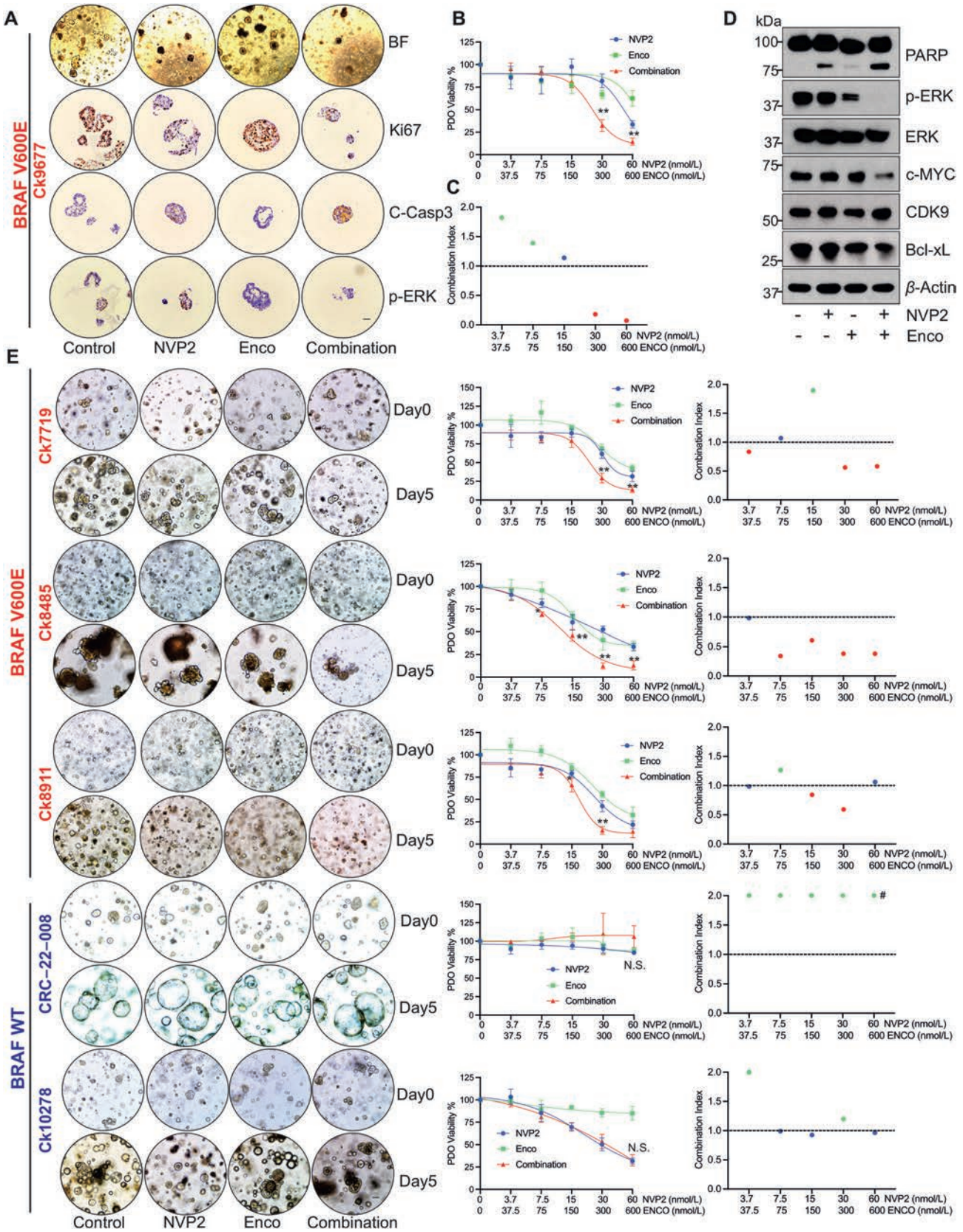

Figure 5 Synergistic effect of CDK9i and BRAFi on the growth of CRC PDOs with *BRAF* ^{V600E} mutation, but not *BRAF* wild type PDOs. (A) IHC staining of PDO CK9677, including Ki-67, cleave caspase-3, and p-ERK. Scale bar: 100 μm. (B) The synergistic effect of CDK9i and/or BRAFi on the growth of CRC PDO CK9677. CK9677 (*BRAF*^{V600E}) PDO were treated with NVP2 and/or Encorafenib for 7 days. PDO viability was determined using CellTiter Glo 3D assay; (C) The combination index was calculated by using the Chou-Talalay method. (D) The synergistic

PDO CK9677, while the co-treatment with CDK9i and BRAFi yielded a stronger cytotoxicity than any single treatment (Fig. 5B). According to the Chou-Talalay method, the combination of CDK9i (30, 60 nmol/L) and BRAFi (300, 600 nmol/L) had a strong synergy (CI $<$ 0.5, Fig. 5C). To further investigate this combination on the alteration of cancer signaling networks, the expression of cleaved PARP, p-ERK, CDK9, c-MYC and Bcl-xL were determined by immunoblot analysis (Fig. 5D). Consistent with our RPPA result, CDK9i in combination with BRAFi synergistically inhibited p-ERK, c-MYC, Bcl-xL, and enhanced the expression of PARP cleavage. To enhance the rigor of our findings in additional patient-derived models, 3 more *BRAF*^{V600E} mutant PDOs (CK7719; CK8485; CK8911) as well as 3 wild-type *BRAF* (CRC-22-008; CRC-22-007; CK10278) PDOs were used. As seen in Fig. 5E and Supporting Information Fig. S11, the synergistic effect between CDK9i and BRAFi was observed in *BRAF*^{V600E} mutant PDOs, while there is non-synergy of this drug combination in *BRAF* wild-type PDOs. Taken together, our results demonstrated that CDK9i synergistically suppressed BRAF/MEK/ERK signaling and induced apoptosis in *BRAF* ^{V600E} mutant CRC PDOs.

3.6. CDK9i sensitizes the in vivo therapeutic efficacy of BRAFi in RKO-xenograft and PDX with BRAF^{V600E}

Given the potent synergistic effect of CDK9i and BRAFi in CRC cells and PDOs, the efficacy of CDK9i and/or BRAFi was further investigated in RKO xenograft and *BRAF*^{V600E} mutant PDX mice models. As seen in Fig. 6A and B, the monotherapy treatment with BRAFi (Encorafenib 10 mg/kg) did not significantly suppress tumor growth ($P = 0.13$), while monotherapy CDK9i (8 mg/kg) alone only led to weak antitumor activity as compared to the control group. Of note, the co-administration of CDK9i and BRAFi resulted in a significant reduction of tumor volume (78%, $P < 0.001$) and tumor weight (Fig. 6C). No significant change in mice body weight was observed, even in the combination group (Fig. 6D). Ki-67 and TUNEL were used as biomarkers of proliferation and apoptosis, respectively. Co-treatment with CDK9i and BRAFi resulted in a greater reduction in Ki-67 expression than any single treatment (Fig. 6E and F). Meanwhile, CDK9i in combination with BRAFi resulted in significantly increased TUNEL-positive staining. Moreover, expression levels of p-ERK were measured. We observed an enhanced inhibition of p-ERK expression in the combination group, which correlated with our *in vitro* results.

To test the antitumor activity in a clinically relevant model *in vivo*, a *BRAF* ^{V600E} mutant PDX was used to investigate the therapeutic efficacy of this combination. On Day 13, the tumor volume of the control group reached $\sim$2000 mm^3, and the tumor volume of CDK9i (NVP2 8 mg/kg) and BRAFi (Encorafenib 10 mg/kg) groups were decreased by 40.4% and 28.0%, respectively, as compared to control. Moreover, the tumor volume of the combination group was markedly reduced by 73.9% ($P < 0.001$). The mice in the CDK9i, BRAFi, and combination groups were continually treated for one more week, during which the co-treatment with CDK9i and BRAFi exerted a more synergistic antitumor activity as compared to the single agent treatments (Fig. 6G). As with the RKO xenograft, there were no significant body weight changes in all treatment groups (Fig. 6H). The therapeutic response to drug treatment within PDX tumors was also measured. As seen in Fig. 6I and J, the combination of CDK9i and BRAFi synergistically blocked the p-ERK signal which is consistent with our *in vitro* and PDO results. MCL-1 and c-MYC were significantly suppressed by the co-treatment of CDK9i and BRAFi. In addition, PDX tumors were examined for biomarkers of growth and apoptosis, including Ki-67, TUNEL and p-S6. The combination of CDK9i and BRAFi resulted in a significant reduction of Ki-67 and p-S6 expression and an increase of TUNEL positive staining (Fig. 6K and L). These results are consistent with data from our CDX and PDO models. Overall, our study showed synergy between BRAFi and CDK9i in multiple *in vivo* models of CRC including a clinically relevant PDX, consistent with our *in vitro* results. In addition, the efficacy of CDK9i and BRAFi on the growth of a *BRAF* WT PDX was evaluated. Although CDK9i exhibited modest antitumor activity (tumor size reduced by 36.0%), there was no additional anti-tumor effect from combining with BRAFi (Fig. 6M and N, CDK9i *vs.* CDK9i + BRAFi, $P > 0.05$).

3.7. CDK9i in combination with BRAFi exerts synergistic effect and enhanced therapeutic response in chemoresistant CRC

Most recently, BRAFi (Encorafenib) in combination with Cetuximab and mFOLFOX6 has been approved for the treatment of mCRC patients with *BRAF*^{V600E} in the first line, based on results from the BREAKWATER trial (NCT04607421)[28]. Unfortunately, chemoresistance remains an obstacle for the treatment of mCRC. To address this, we examined the therapeutic efficacy of BRAFi in combination with CDK9i in a chemoresistant CRC model (RKO-5FUR10). As seen Fig. 7A and B, The RKO-5FUR10 cells exhibited 5-FU-resistant phenotype, as compared to the parental cells. Moreover, the efficacy of chemotherapy (FOLFOX) in combination with BRAFi were investigated in RKO and RKO-5FUR10 cells. The synergistic effect of FOLFOX and BRAFi was only observed in RKO cells, but not RKO-5FUR10 cells (Fig. 7C). Our results suggest that RKO-5FUR10 cells are resistant to the combination of chemotherapy and BRAFi. Of note, CDK9i in combination with BRAFi resulted in a strong synergistic effect (CI $<$ 0.5) on the growth of chemo-resistant CRC cells (Fig. 7D−F). We observed a similar effect on cancer signaling pathways after CDK9i and BRAFi treatment in chemoresistant CRC cells as compared to chemo-sensitive cells. This drug combination significantly suppressed the BRAF/MEK/ERK/S6 and AKT/mTOR/4E-BP1 pathways, inhibited downstream effectors (c-MYC, MCL-1) of CDK9 and pro-apoptotic BCL2 members, and enhanced PARP cleavage, cleaved caspase-3 and BAX in RKO-5FUR10 cells (Fig. 7G and H). In addition to the chemoresistant CRC cells, a 5-FU-resistant CRC PDO (CK7719, Fig. 7I) was used to evaluate the combination of CDK9i and BRAFi. As seen in Fig. 7J, CDK9i significantly enhanced the

effect of CDK9i and BRAFi on suppressing p-ERK/p-S6 and C-Myc, inducing cleaved PARP in PDO. (E) Therapeutic response to the CDK9i in combination with BRAFi in multiple PDOs, including *BRAF*^{V600E} (CK7719, CK8485, CK8911); *BRAF* WT (CRC-22-008 and CK10278). The organoids were exposed to CDK9i and/BRAFi for 5 days, and images were shown at Day 0 and Day 5; After 7 days treatment, the growth of PDOs were determined using CellTiter Glo 3D assay. Values in the graph represent the mean ± SD from 3 to 5 independent experiments. **P*<0.05*, ***P* < 0.01; N.S. (not significant) NVP2 *vs.* Combination; # means CI > 2.

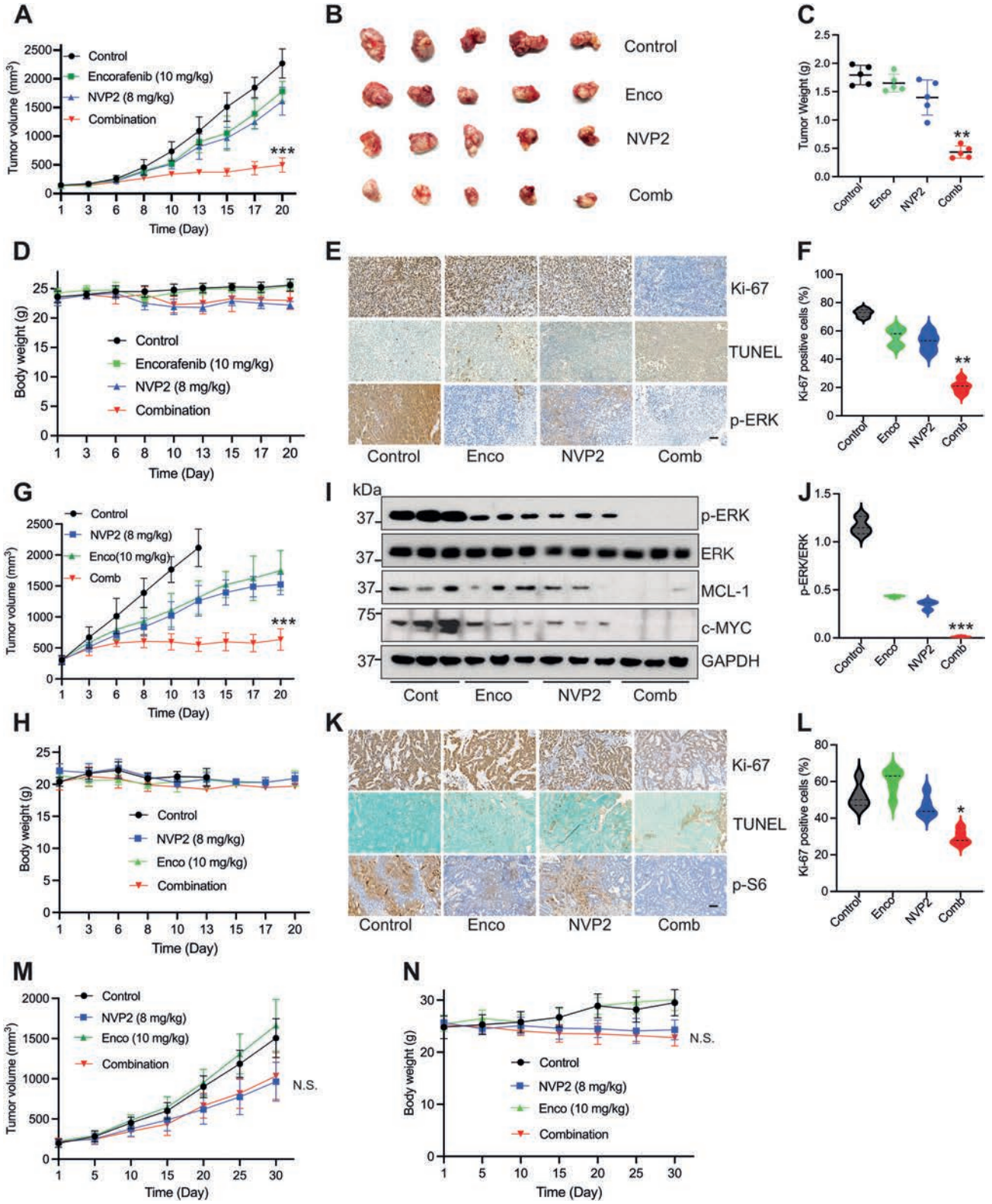

Figure 6 CDK9i sensitizes the *in vivo* therapeutic efficacy of BRAFi in RKO-xenograft and PDX with $BRAF^{V600E}$. The synergistic effect of Encorafenib and NVP2 on tumor growth. Athymic nude mice bearing RKO tumor xenografts were administered 5 daily/week vehicle control, Encorafenib (10 mg/kg), NVP2 (8 mg/kg), and combination orally for 3 weeks (5 mice per group). (A, D) Tumor volume and body weight were measured 3 times per week. (B) The image of excised tumor and tumor weights (C) after treatment with CDK9i and/or BRAFi. (E, F) Tumors were fixed in formalin and paraffin-embedded. Slides were stained for Ki-67, TUNEL and p-ERK; NOD-SCID mice bearing $BRAF^{V600E}$ mutant PDX model. After tumor size reached ~300 mm^3, the mice were treated with vehicle control, NPV2 and/or Encoranfenib orally for 5 days/week for 20 days (5 mice/group). (G) Tumor volume and body weight (H) were monitored 3 times per week; (I, J) protein expression in $BRAF^{V600E}$

effect of BRAFi on suppressing p-ERK. Overall, our results suggest that the synergistic effect between CDK9i and BRAFi might function even in chemo-resistant CRC patients.

4. Discussion

Due to intrinsic resistance, the therapeutic efficacy of BRAFi in mCRC patients with mutant *BRAF* ^{V600E} is often limited, and the clinical response to BRAFi monotherapy is only ~5%[29]. Of note, the molecular mechanism of *BRAF* ^{V600E} mutant mCRC is more complex than melanoma. In CRC, BRAFi causes an initial suppression of MAPK signaling which leads to a reduction of ERK-mediated negative feedback[30]. These biological events impact the several upstream pathways, including RTK-mediated RAS activation and the recruitment of other RAF kinases (CRAF), which all contribute to paradoxical activation of the MAPK pathways in mCRC[31-33]. In particular, BRAFi results in a rapid feedback activation of EGFR, a dominant RTK in colon cancer. Reactivation of ERK through EGFR-mediated activation of RAS and CRAF has been found to maintain tumor growth in the presence of BRAFi[14,34]. CDC25C has also been identified as playing a key role in the activation of EGFR[34]. Since enhanced EGFR signaling is responsible for resistance to BRAFi monotherapy, blockade of EGFR exhibited strong synergy in combination with BRAFi in *BRAF* mutant CRC models. Based on this resistance mechanism, the FDA approved Encorafenib (BRAFi) in combination with Cetuximab (EGFRi) for mCRC with *BRAF*^{V600E} mutation[5]. More recently, on December 20th, 2024, the FDA granted accelerated approval to Encorafenib plus Cetuximab and mFOLFOX6 for the first-line treatment of patients with *BRAF*^{V600E} mutant mCRC[28]. While these recent approvals are promising in bringing targeted therapies to patients in earlier lines of treatment, they also highlight the fact that durability and drug resistance remain a significant issue for *BRAF*^{V600E} mutant CRC. For example, the median PFS for patients who received Encorafenib plus Cetuximab and mFOLFOX6 in the BREAKWATER study was 12.8 months[20]. While this PFS is a significant improvement over the previous standard of care (7.1 months), the finding also suggests that nearly half of mCRC patients with *BRAF*^{V600E} who receive the most up-to-date regimen will be resistant to both BRAFi and chemotherapy within a year of starting treatment. Thus, there is ample unmet need for novel therapies that can overcome either *de novo* or acquired therapeutic resistance.

In this study, we aimed to discover novel agents/targets that can sensitize the therapeutic response of BRAFi in intrinsically resistant mCRC. We utilized HT-29 and RKO cell lines due to their intrinsic resistance to BRAFi therapy (Fig. 1A−C). The mechanisms of clinical resistance to BRAFi therapies in CRC have been heterogeneous, but generally involve genomic or proteomic changes that maintain active MAPK signaling[35]. Our results indicate that HT-29 and RKO recapitulate this general mechanism of resistance quite well, since p-ERK signaling was poorly inhibited by BRAFi's in these two cell lines as compared to Colo205 (Fig. 2D and E). CDK9 inhibitors were identified as top candidate agents using phenotypic HTS of a kinase inhibitor library. CDK9 is now emerging as a potential therapeutic target for cancers[36], with approximately 20 CDK9 inhibitors entering various stages of clinical trials, such as AZD4573, NVP2, BAY1251152, KB-0742, Zotiraciclib, etc[37-41]. In addition, high-level expression of CDK9 was correlated with tumorigenesis and poor clinical outcomes[22], including in mCRC. Consistently, the protein expression level of CDK9 in human CRC cells is much higher than that in normal human epithelial colon cells (Fig. 2F). Using the TCGA database of human CRCs, there is no significant difference of *CDK9* mRNA expression in CRC patients with wildtype *BRAF* and mutant *BRAF* ($P = 0.4808$). Of note, CPTAC (Clinical Proteomic Tumor Analysis Consortium) analysis demonstrated that CDK9 protein expression in BRAF V600E mutant CRC patient is higher than that in CRC patients with wildtype *BRAF* ($P = 0.0003$, Supporting Information Fig. S12). Previous studies showed that CDK9/Src kinase interplay contributes to ERK phosphorylation. Meanwhile, our RNA-seq data suggest that CDK9i down-regulated MAPK signaling. It is known that feedback activation of ERK leads to poor response to Vemurafenib[14]. CDK9, a core subunit of P-TEFb (positive transcription elongation factor b), regulates transcriptional elongation by releasing RNA polymerase II from promoter-proximal pausing, with diverse downstream targets, meaning that CDK9i may be uniquely capable of suppressing multiple important cancer driver pathways. With this in mind, we examined the synergistic effect of CDK9i and BRAFi on the p-ERK signal[42]. CDK9i can significantly enhance the efficacy of BRAFi on long-term suppression of p-ERK in CRC cells, PDOs, and PDX with *BRAF*^{V600E} mutation. In addition, genetic alterations in the PI3K/AKT have been associated with cancer intrinsic resistance. PI3K/AKT is usually much more activated in mCRC, as compared to melanoma[43]. In a phase II trial conducted with BRAFi (Dabrafenib) and MEKi (Trametinib), one case achieved a complete response among five patients with PI3KCA mutations. The combination of Encorafenib, Cetuximab, and Alpelisib has shown clinical benefit in *BRAF*-mutant mCRC[44]. Our RPPA data showed that the combination of CDK9i and BRAFi also suppressed the AKT/mTOR/4E-BP1 pathway. Thus, CDK9i in combination with BRAFi synergistically suppressed two critical cancer driver pathways, and the potential feedback activation of ERK was significantly blocked. CDK9, as a promoter of transcriptional elongation, also regulates the expression of anti-apoptotic BCL-2 members (BCL-2, MCL-1, and BCL-XL)[45]. In response to apoptosis, CDK9 also promotes the expression and/or activity of oncogenic transcription factors such as c-MYC[46]. Herein, the combination of CDK9i and BRAFi yielded a stronger reduction of MCL-1, BCL-2, BCL-XL, and c-MYC as compared to monotherapy. Overall, our findings suggest that CDK9 inhibition in CRC causes widespread transcriptional suppression that impacts multiple oncogenic pathways, consistent with studies in other tumors[47-49]. However, we herein characterize a unique, synergistic relationship between CDK9 inhibition and MAPK pathway inhibition in CRC, nominating a novel combination treatment approach. This might be due to the overall

PDX was determined after 20 days of CDK9i and/or BRAFi treatment. Tumors were harvested 2 h after the last dose. (K, L) Tumors were fixed in formalin and paraffin-embedded. Slides were stained for Ki-67, TUNEL and p-S6. Scale bar: 50 μm; After tumor size reached ~200 mm^3, the mice bearing *BRAF* WT CRC tumor (CM0050) were treated with vehicle control, NPV2 and/or Encorafenib orally 5 days/week for 30 days. (M) Tumor size and (N) body weight of PDX mice were monitored; Values in the graph represent the mean ± SD. ***$P < 0.001$ CDK9i (NVP2) *vs.* Combination (NVP2+Enco); N.S. $P > 0.05$ CDK9i (NVP2) *vs.* Combination (NVP2+Enco).

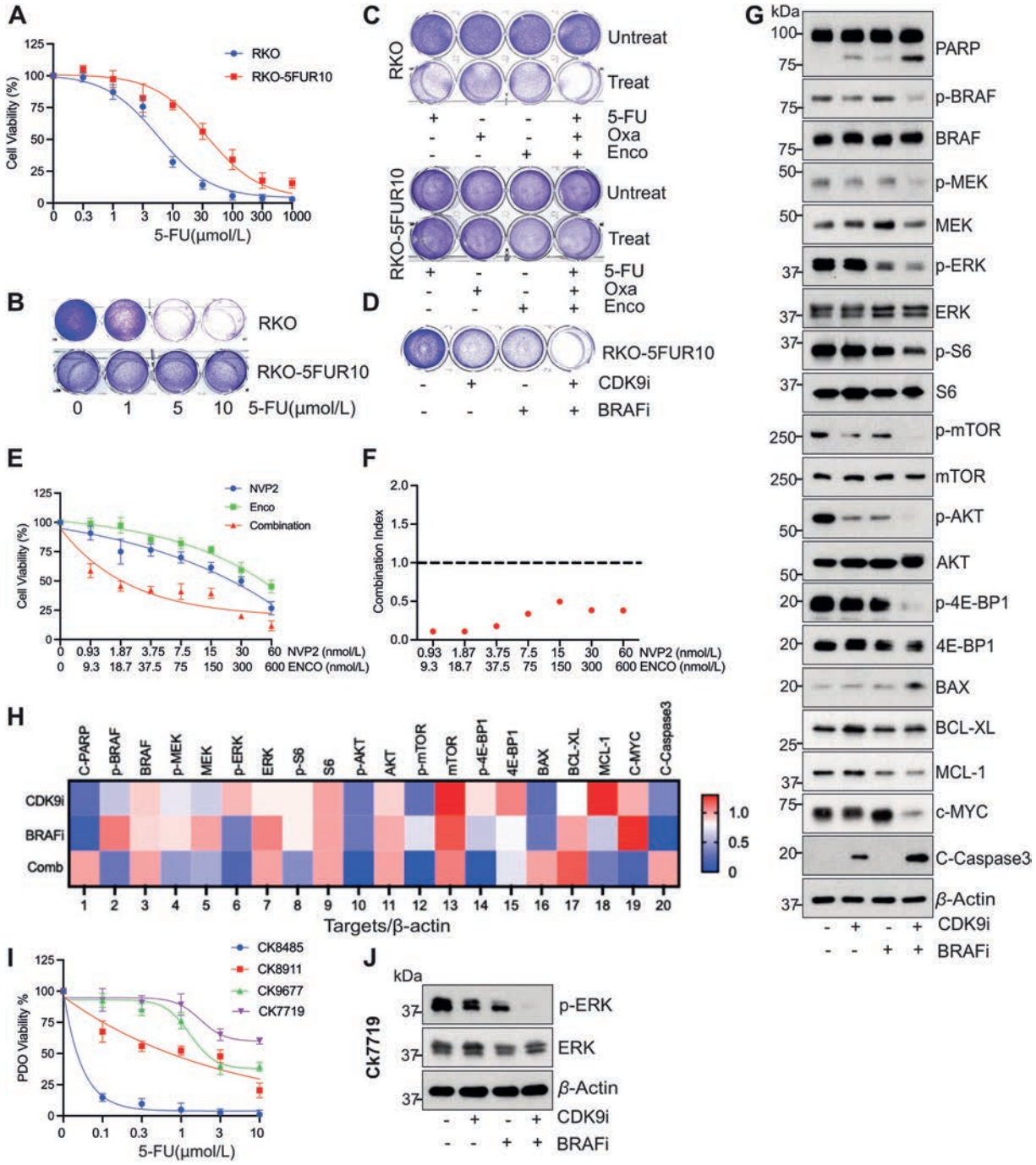

Figure 7 CDK9i in combination with BRAFi exerts synergistic effect in chemoresistant CRC. (A) The effect of 5-FU on the growth of RKO-5FUR10 and parental cells. RKO and RKO-5FUR10 cells were treated with 5-FU for 72 h, and the cell viability was determined by MTS assay; (B) The cytotoxic effect 5-FU on the survival of RKO and RKO-5FUR10 cells; RKO or RKO-5FUR10 cells were incubated with 5-FU for 48 h, the living cells were stained by crystal violet. (C) The efficacy of FOLFOX in combination with BRAFi on the growth of RKO and RKO-5FUR10 cells; (D, E) The synergistic effect of CDK9i and BRAFi on the growth of RKO-5FUR10 cells. RKO-5FUR10 cells were treated with CDK9i (NVP2) and/or BRAFi for 48 or 72 h. Cell growth was visualized and quantified by crystal violet and the MTS assay, respectively. (F) Data from 3 to 5 independent experiments were used to calculate the Combination Index (CI). (G, H) The effect of CDK9i and BRAFi on alteration of cancer signaling network, including BRAF/MEK/ERK/S6; AKT/mTOR/4E-BP1 and downstream effectors of CDK9. RKO-5FUR10 cells were treated with CDK9i and/or BRAFi for 24 h, the expression level of relevant target proteins was determined by immunoblot analysis. (I) The cytotoxic effect of 5-FU on the growth of PDOs with $BRAF^{V600E}$. After treatment with 5-FU for 7 days, the viability of PDOs was determined by Cell Titer Glo 3D. (J) The synergistic effect of CDK9i and BRAFi on suppressing p-ERK in 5-FU-resistant PDO (CK7719); A representative image was shown from 3 independent experiments.

dependence of CRC on MAPK signaling to drive cancer metabolism and growth, including transcriptional activation. Accordingly, CDK9i's may also enhance the activity of KRAS inhibitors in KRAS-mutant CRC, which is the topic of our separate study. Additional functional genetic studies to test the role of the multiple potential downstream targets of CDK9i in CRC are planned.

In principle, combination therapy holds several advantages over monotherapy. First, our study has demonstrated the synergistic anti-tumor effects of combining BRAFi and CDK9i. Second, by combining multiple agents with synergistic effects against the tumor, we hope that lower doses of each individual agent are sufficient to induce a potent therapeutic effect. Decreasing the doses may also permit the use of a drug at a more tolerable or safer dose. In our study, we observed no significant body weight change in mice treated with CDK9i and BRAFi, suggesting that there should be a reasonable therapeutic index for such a combination. In the first-in-human phase I study of the CDK9i, VIP152/BAY1251152, the PK analysis showed that plasma drug levels exceeded 200 nmol/L for more than 12 h in patients who took the MTD[39]. In our study, such a concentration of BAY1251152 was sufficient to induce potent synergistic tumor suppression. This analysis suggests that the CDK9i drug exposure necessary for synergy with BRAFi can be achieved in humans. The dose limiting toxicity of BAY1251152 monotherapy was neutropenia. The most significant toxicities of Encorafenib are fatigue, nausea, and arthralgias. In this study, lower dose of CDK9i and Encorafenib exhibited a synergistic antitumor activity in CDX and PDX models, and no evident toxicity was observed. It is possible that CDK9i and BRAFi toxicity profiles are non-overlapping, suggesting that a therapeutic index for CDK9i plus BRAFi should be tolerable to CRC patients.

Historically, $BRAF^{V600E}$ mutant mCRC had a poor response to standard therapies, such as 5-FU-based chemotherapy. To test the effect of CDK9i in combination with BRAFi on 5-FU-resistant *BRAF* mutant CRC models, RKO-5FUR10 cells were acquired. the IC_{50} of 5-FU in resistant cells was $\sim$30 μmol/L, and 6-fold higher than that in parental RKO cells. Moreover, the synergistic benefit of CDK9i and BRAFi was confirmed in RKO-5FUR10 cells. These findings suggest that CDK9i in combination with BRAFi could be effective against chemoresistant mCRC (Fig. 7D−F). In further support of this finding, we demonstrated that even a chemo-resistant PDO (CK7719) was susceptible to treatment with BRAFi and CDK9i (Figs. 5E and 7I and J). In addition to sensitization of the intrinsic resistant and acquired resistant CRC models, CDK9i can also enhance the efficacy of low doses of BRAFi (1 nmol/L) against Colo205 (a BRAFi-sensitive cell line, Supporting Information Fig. S13). Recent studies showed that CDK9 expression is induced upon inhibition of P-TEFb activity, a process dependent on BRD4[50]. Given that CDK9i could sensitize the efficacy of BRAFi, it is possible that BRD4 inhibitor (JQ-1) in combination with BRAFi also yields a synergistic effect. As seen in Supporting Information Fig. S14, JQ-1 combined with BRAFi (Encorafenib) synergistically suppressed the growth of RKO cells. Thus, BRD4i could also be a potential target for sensitization of BRAFi-resistant CRC. Given the ability of CDK9i + BRAFi to synergistically treat CRC models that are resistant to BRAFi's and chemotherapy, this combination holds promise as a potential salvage treatment for patients who have progressed on first-line FOLFOX + Encorafenib + Cetuximab. Future work will focus on testing the efficacy of CDK9i combinations in additional patient-derived models that are resistant to both chemo- and targeted therapies.

In CRC, PDOs and PDXs have been studied as potential models for precision oncology. PDOs are capable of predicting responses to standard therapies in mCRC patients with 100% sensitivity and 93% specificity[51]. PDOs, as a superior preclinical model, have inherent heterogeneity and long-term stability, as compared to cancer cell lines. PDOs have been shown to predict clinical outcomes is better than biomarker panels alone[52]. In our study, we validated the synergistic effect of CDK9i and BRAFi in 4 unique $BRAF^{V600E}$ mutant PDOs and a PDX model. Furthermore, we determined the lack of synergy in 3 unique *BRAF* WT PDOs and a *BRAF* WT PDX. We used subcutaneous flank tumor xenografts in our study. One method that could enhance our findings is to use orthotopic models. Orthotopic models allow tumors to grow within their organ of origin, better replicating the complex organ-specific tumor microenvironment (TME) observed in human patients. Orthotopic models represent a more disease-relevant preclinical approach compared to their subcutaneous counterparts, as they more reliably preserve the intrinsic tissue structure and complexities of patient tumors *in situ*. Orthotopic tumor models can generate more patient-relevant pharmacodynamic profiles for targeted therapies and immunotherapeutic agents, which provide more relevant efficacy and drug resistance profiles.

Encorafenib, a highly selective ATP-competitive BRAF inhibitor, exhibited antitumor activity against $BRAF^{V600E}$ mutant cancers and had longer pharmacodynamic activity than other *BRAF* inhibitors. To determine the specificity of our BRAFi + CDK9i combinations against $BRAF^{V600E}$ mutant tumors, we also studied their efficacy against BRAF WT models. As expected due to a lack of $BRAF^{V600E}$ mutation, Encorafenib alone did not affect the tumor growth of the *BRAF* WT PDX. Furthermore, NVP2 and Encorafenib had a non-synergistic effect against the BRAF WT PDX, consistent with the lack of BRAF V600E mutation. Together, our results strongly suggest that CDK9i and BRAFi combinations are a promising therapeutic approach for BRAFi and chemo-resistant $BRAF^{V600E}$ CRC.

In summary, CDK9i in combination with BRAFi led to synergistic therapeutic responses in CRC cells, PDOs, and PDX with $BRAF^{V600E}$ mutation, through blockage of BRAF/MEK/ERK/S6 and AKT/mTOR/4E-BP1. Targeting CDK9-mediated transcriptional elongation appears to be a promising combination strategy for BRAFi-based treatment in mCRC, even in chemoresistant mCRC. These findings provide the rationale for clinical testing of CDK9i plus BRAFi in CRC, while also facilitating potential new hypotheses about how to use CDK9 inhibitors in combination treatments.

Acknowledgments

This project was supported by the Montefiore Einstein Comprehensive Cancer Center grant (NCI P30CA013330, USA, Edward Chu). FFPE specimen processing, slide cutting, and staining was conducted by Laura Ramkissoon of the Albert Einstein College of Medicine Histology and Comparative Pathology Facility, which is partially funded by NCI grant P30CA013330. Slide scanning was conducted by Hillary Guzik, Rotem Alon and Vera DesMarais, of the Albert Einstein Analytical Imaging Facility (AIF) core. The 3DHistech Pannoramic 250 digital slide scanner is housed in the AIF and was purchased with NIH grant SIG S10OD026852-01A1. The AIF is partially funded by NCI grant P30CA013330. Flow cytometry was conducted in the Albert Einstein Flow Cytometry Core Facility which is supported in part by the NIH SIG

1S10OD026833-01 and NCI grant P30CA013330. The Functional Proteomics Reverse Phase Protein Array Core was supported in part by The University of Texas MD Anderson Cancer Center, P30CA016672 and R50CA221675. Graphical abstract was created in BioRender. (Wei, N. (2026) https://BioRender.com/0epcqrk).

Author contributions

Ning Wei: Conceptualization, data curation, supervision, investigation, methodology, writing−original draft and editing. Natalie Thielen: Methodology, data curation, software, investigation, validation, writing−original draft. Mahshid Mohammadi: Resources, methodology. Muzaffer Ahmed Bhat: Investigation, methodology. Terence Li: methodology. Yan Sun: Data curation, investigation. Seiya Kitamura: Methodology. Chaoyuan Kuang: Conceptualization, funding acquisition, supervision, writing-review and editing. Edward Chu: Conceptualization, supervision, funding acquisition, writing−review and editing.

Conflicts of interest

CK has the following disclosures: Teiko (consultant), Seattle Genetics (advisory board), Loki (collaboration/funding), BMS (advisory board), Guardant Health (advisory board). The remaining authors declare that they have no known competing financial interests or personal relationships that could have appeared to influence the work reported in this paper.

Supporting information

Supporting information to this article can be found online at https://doi.org/10.1016/j.apsb.2026.05.008.

References

1. Bray F, Laversanne M, Sung H, Ferlay J, Siegel RL, Soerjomataram I, et al. Global cancer statistics 2022: GLOBOCAN estimates of incidence and mortality worldwide for 36 cancers in 185 countries. *CA Cancer J Clin* 2024;**74**:229−63.
2. Siegel RL, Kratzer TB, Giaquinto AN, Sung H, Jemal A. Cancer statistics, 2025. *CA Cancer J Clin* 2025;**75**:10−45.
3. Davies H, Bignell GR, Cox C, Stephens P, Edkins S, Clegg S, et al. Mutations of the BRAF gene in human cancer. *Nature* 2002;**417**: 949−54.
4. Chu E. An update on the current and emerging targeted agents in metastatic colorectal cancer. *Clin Colorectal Cancer* 2012;**11**:1−13.
5. Taieb J, Lapeyre-Prost A, Laurent Puig P, Zaanan A. Exploring the best treatment options for BRAF-mutant metastatic colon cancer. *Br J Cancer* 2019;**121**:434−42.
6. Schirripa M, Biason P, Lonardi S, Pella N, Pino MS, Urbano F, et al. Class 1, 2, and 3 BRAF-mutated metastatic colorectal cancer: a detailed clinical, pathologic, and molecular characterization. *Clin Cancer Res* 2019;**25**:3954−61.
7. Barras D, Missiaglia E, Wirapati P, Sieber OM, Jorissen RN, Love C, et al. BRAF V600E mutant colorectal cancer subtypes based on gene expression. *Clin Cancer Res* 2017;**23**:104−15.
8. Cremolini C, Di Bartolomeo M, Amatu A, Antoniotti C, Moretto R, Berenato R, et al. BRAF codons 594 and 596 mutations identify a new molecular subtype of metastatic colorectal cancer at favorable prognosis. *Ann Oncol* 2015;**26**:2092−7.
9. Yao Z, Yaeger R, Rodrik-Outmezguine VS, Tao A, Torres NM, Chang MT, et al. Tumours with class 3 BRAF mutants are sensitive to the inhibition of activated RAS. *Nature* 2017;**548**:234−8.
10. Leach JDG, Vlahov N, Tsantoulis P, Ridgway RA, Flanagan DJ, Gilroy K, et al. Oncogenic BRAF, unrestrained by TGFbeta−receptor signalling, drives right-sided colonic tumorigenesis. *Nat Commun* 2021;**12**:3464.
11. Hanrahan AJ, Solit DB. BRAF mutations: the discovery of allele- and lineage-specific differences. *Cancer Res* 2022;**82**:12−4.
12. Hanrahan AJ, Chen Z, Rosen N, Solit DB. BRAF—a tumour-agnostic drug target with lineage-specific dependencies. *Nat Rev Clin Oncol* 2024;**21**:224−47.
13. Martinelli E, Cremolini C, Mazard T, Vidal J, Virchow I, Tougeron D, et al. Real-world first-line treatment of patients with BRAF(V600E)-mutant metastatic colorectal cancer: the CAPSTAN CRC study. *ESMO Open* 2022;**7**:100603.
14. Corcoran RB, Ebi H, Turke AB, Coffee EM, Nishino M, Cogdill AP, et al. EGFR-mediated re-activation of MAPK signaling contributes to insensitivity of BRAF mutant colorectal cancers to RAF inhibition with vemurafenib. *Cancer Discov* 2012;**2**:227−35.
15. Hafliger E, Boccaccino A, Lapeyre-Prost A, Perret A, Gallois C, Antista M, et al. Encorafenib plus cetuximab treatment in BRAF V600E-mutated metastatic colorectal cancer patients pre-treated with an anti-EGFR: an AGEO-GONO case series. *Eur J Cancer* 2022;**168**: 34−40.
16. Kopetz S, Grothey A, Yaeger R, Van Cutsem E, Desai J, Yoshino T, et al. Encorafenib, binimetinib, and cetuximab in BRAF V600E-mutated colorectal cancer. *N Engl J Med* 2019;**381**:1632−43.
17. Tabernero J, Grothey A, Van Cutsem E, Yaeger R, Wasan H, Yoshino T, et al. Encorafenib plus cetuximab as a new standard of care for previously treated BRAF V600E-mutant metastatic colorectal cancer: updated survival results and subgroup analyses from the BEACON study. *J Clin Oncol* 2021;**39**:273−84.
18. Napolitano S, Woods M, Lee HM, De Falco V, Martini G, Della Corte CM, et al. Antitumor efficacy of dual blockade with encorafenib + cetuximab in combination with chemotherapy in human BRAFV600E-mutant colorectal cancer. *Clin Cancer Res* 2023;**29**: 2299−309.
19. Lézard L. US FDA approves Pfizer's BRAFTOVI® combination regimen as first-line treatment of BRAF V600E-mutant metastatic colorectal cancer. Available from: https://www.pfizer.com/news/press-release/press-release-detail/us-fda-approves-pfizers-braftovir-combination-regimen-first.
20. Elez E, Yoshino T, Shen L, Lonardi S, Van Cutsem E, Eng C, et al. Encorafenib, cetuximab, and mFOLFOX6 in BRAF-mutated colorectal cancer. *N Engl J Med* 2025;**392**:2425−37.
21. Atkins MB, Lee SJ, Chmielowski B, Tarhini AA, Cohen GI, Truong TG, et al. Combination dabrafenib and trametinib *versus* combination nivolumab and ipilimumab for patients with advanced BRAF-mutant melanoma: the DREAMseq trial-ECOG-ACRIN EA6134. *J Clin Oncol* 2023;**41**:186−97.
22. Mo C, Wei N, Li T, Ahmed Bhat M, Mohammadi M, Kuang C. CDK9 inhibitors for the treatment of solid tumors. *Biochem Pharmacol* 2024; **229**:116470.
23. Somarelli JA, Roghani RS, Moghaddam AS, Thomas BC, Rupprecht G, Ware KE, et al. A precision medicine drug discovery pipeline identifies combined CDK2 and 9 inhibition as a novel therapeutic strategy in colorectal cancer. *Mol Cancer Ther* 2020;**19**: 2516−27.
24. Liu H, Liu H, Zhou Z, Chung J, Zhang G, Chang J, et al. Scutellaria baicalensis enhances 5-fluorouracil-based chemotherapy *via* inhibition of proliferative signaling pathways. *Cell Commun Signal* 2023;**21**:147.
25. Wei N, Li J, Fang C, Chang J, Xirou V, Syrigos NK, et al. Targeting colon cancer with the novel STAT3 inhibitor bruceantinol. *Oncogene* 2019;**38**:1676−87.
26. Wei N, Burnett J, Crocker DL, Huang Y, Li S, Wipf P, et al. Quassinoid analogs exert potent antitumor activity *via* reversible protein biosynthesis inhibition in human colorectal cancer. *Biochem Pharmacol* 2023;**212**:115564.
27. Chou TC. Drug combination studies and their synergy quantification using the Chou-Talalay method. *Cancer Res* 2010;**70**:440−6.

28. Kopetz S, Yoshino T, Van Cutsem E, Eng C, Kim TW, Wasan HS, et al. Encorafenib, cetuximab and chemotherapy in BRAF-mutant colorectal cancer: a randomized phase 3 trial. *Nat Med* 2025;**31**:901−8.
29. Lee HM, Morris V, Napolitano S, Kopetz S. Evolving strategies for the management of BRAF-mutant metastatic colorectal cancer. *Oncology (Williston Park)* 2019;**33**:206−11.
30. Dienstmann R, Vermeulen L, Guinney J, Kopetz S, Tejpar S, Tabernero J. Consensus molecular subtypes and the evolution of precision medicine in colorectal cancer. *Nat Rev Cancer* 2017;**17**:79−92.
31. Terrell EM, Morrison DK. Ras-mediated activation of the Raf family kinases. *Cold Spring Harb Perspect Med* 2019;**9**:a033746.
32. Wang P, Laster K, Jia X, Dong Z, Liu K. Targeting CRAF kinase in anticancer therapy: progress and opportunities. *Mol Cancer* 2023;**22**:208.
33. Bahar ME, Kim HJ, Kim DR. Targeting the RAS/RAF/MAPK pathway for cancer therapy: from mechanism to clinical studies. *Signal Transduct Target Ther* 2023;**8**:455.
34. Prahallad A, Sun C, Huang S, Di Nicolantonio F, Salazar R, Zecchin D, et al. Unresponsiveness of colon cancer to BRAF(V600E) inhibition through feedback activation of EGFR. *Nature* 2012;**483**:100−3.
35. Ahronian LG, Sennott EM, Van Allen EM, Wagle N, Kwak EL, Faris JE, et al. Clinical acquired resistance to RAF inhibitor combinations in BRAF-mutant colorectal cancer through MAPK pathway alterations. *Cancer Discov* 2015;**5**:358−67.
36. Mandal R, Becker S, Strebhardt K. Targeting CDK9 for anti-cancer therapeutics. *Cancers (Basel)* 2021;**13**:2181.
37. Cidado J, Boiko S, Proia T, Ferguson D, Criscione SW, San Martin M, et al. AZD4573 is a highly selective CDK9 inhibitor that suppresses MCL-1 and induces apoptosis in hematologic cancer cells. *Clin Cancer Res* 2020;**26**:922−34.
38. Olson CM, Jiang B, Erb MA, Liang Y, Doctor ZM, Zhang Z, et al. Pharmacological perturbation of CDK9 using selective CDK9 inhibition or degradation. *Nat Chem Biol* 2018;**14**:163−70.
39. Diamond JR, Boni V, Lim E, Nowakowski G, Cordoba R, Morillo D, et al. First-in-human dose-escalation study of cyclin-dependent kinase 9 inhibitor VIP152 in patients with advanced malignancies shows early signs of clinical efficacy. *Clin Cancer Res* 2022;**28**:1285−93.
40. Freeman DB, Hopkins TD, Mikochik PJ, Vacca JP, Gao H, Naylor-Olsen A, et al. Discovery of KB-0742, a potent, selective, orally bioavailable small molecule inhibitor of CDK9 for MYC-dependent cancers. *J Med Chem* 2023;**66**:15629−47.
41. Le Rhun E, Gorlia T, Felsberg J, Jongen J, Maurage CA, Ducray F, et al. Zotiraciclib (TG02) for newly diagnosed glioblastoma in the elderly or for recurrent glioblastoma: the EORTC 1608 STEAM trial. *Eur J Cancer* 2024;**198**:113475.
42. Wang Y, Xu L, Ling L, Yao M, Shi S, Yu C, et al. Unraveling the CDK9/PP2A/ERK network in transcriptional pause release and complement activation in KRAS-mutant cancers. *Adv Sci (Weinh)* 2024;**11**:e2404926.
43. Guerrero P, Albarran V, San Roman M, Gonzalez-Merino C, Garcia de Quevedo C, Moreno J, et al. BRAF inhibitors in metastatic colorectal cancer and mechanisms of resistance: a review of the literature. *Cancers (Basel)* 2023;**15**:5243.
44. van Geel R, Tabernero J, Elez E, Bendell JC, Spreafico A, Schuler M, et al. A Phase Ib dose-escalation study of encorafenib and cetuximab with or without alpelisib in metastatic BRAF-mutant colorectal cancer. *Cancer Discov* 2017;**7**:610−9.
45. Inoue-Yamauchi A, Jeng PS, Kim K, Chen HC, Han S, Ganesan YT, et al. Targeting the differential addiction to anti-apoptotic BCL-2 family for cancer therapy. *Nat Commun* 2017;**8**:16078.
46. Vervoort SJ, Welsh SA, Devlin JR, Barbieri E, Knight DA, Offley S, et al. The PP2A−Integrator−CDK9 axis fine-tunes transcription and can be targeted therapeutically in cancer. *Cell* 2021;**184**:3143-62.e32.
47. Zhang H, Pandey S, Travers M, Sun H, Morton G, Madzo J, et al. Targeting CDK9 reactivates epigenetically silenced genes in cancer. *Cell* 2018;**175**:1244-58.e26.
48. Mustafa EH, Laven-Law G, Kikhtyak Z, Nguyen V, Ali S, Pace AA, et al. Selective inhibition of CDK9 in triple negative breast cancer. *Oncogene* 2024;**43**:202−15.
49. Rahman R, Rahaman MH, Hanson AR, Choo N, Xie J, Townley SL, et al. CDK9 inhibition inhibits multiple oncogenic transcriptional and epigenetic pathways in prostate cancer. *Br J Cancer* 2024;**131**:1092−105.
50. Lu H, Xue Y, Yu GK, Arias C, Lin J, Fong S, et al. Compensatory induction of MYC expression by sustained CDK9 inhibition *via* a BRD4-dependent mechanism. *eLife* 2015;**4**:e06535.
51. Li Q, Geng S, Luo H, Wang W, Mo YQ, Luo Q, et al. Signaling pathways involved in colorectal cancer: pathogenesis and targeted therapy. *Signal Transduct Target Ther* 2024;**9**:266.
52. Vlachogiannis G, Hedayat S, Vatsiou A, Jamin Y, Fernandez-Mateos J, Khan K, et al. Patient-derived organoids model treatment response of metastatic gastrointestinal cancers. *Science* 2018;**359**:920−6.